Macromolecules

ARTICLE

pubs.acs.org/Macromolecules

Increasing Lamellar Twisting Frequency with Poly(lactic acid) Segments Incorporation in Poly(trimethylene terephthalate) Ring-Banded Spherulites

Jun Li,[†] Ya Li,[†] Jian Zhou,[†] Jian Yang,[†] Zhiqiang Jiang,[†] Peng Chen,[†] Yuzhong Wang,[‡] Qun Gu,[*,†] and Zongbao Wang[†,*]

[†]Ningbo Key Laboratory of Polymer Materials, Ningbo Institute of Material Technology and Engineering, Chinese Academy of Sciences, Ningbo 315201, China

[‡]Center for Degradable and Flame-Retardant Polymeric Materials (ERCEPM), College of Chemistry, Sichuan University, Chengdu 610064, China

Supporting Information

ABSTRACT: In this study, a series of random poly(trimethylene terephthalate)-*co*-polylactide copolyesters (PTT-*co*-PLA) were synthesized by melting copolycondensation, and the influence of PLA segments on the lamellar twisting frequency of PTT was studied. Etching technology was used to study lamellar morphologies of ring-banded spherulites and distinct images of twisting lamellae in crystalline PTT and PTT-*co*-PLA were observed by scanning electron microscopy. Comparing with PTT homopolymer, ring-banded spherulites in PTT-*co*-PLA have much smaller band spacing and the band spacing decreases sharply with the increase of PLA segments content. It was confirmed by experiments that there are 2-fold reasons for the sharp decrease of band spacing in PTT-*co*-PLA ring-banded spherulites. First, the unbalanced surface stress at the fold surfaces for the PTT lamellar twisting can be intensified by amorphous PLA segments. Second, the thickness of PTT lamellae decreases with the increase of PLA segments content. Both changes significantly enhance the helical twisting frequency of twisted lamellae.

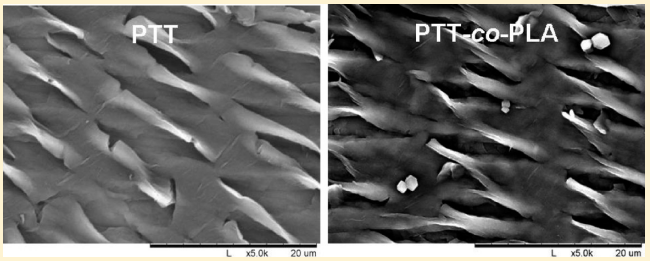

INTRODUCTION

Ring-banded spherulites, as interesting and representative morphological feature of polymer crystalline aggregates, have been attracting considerable attention for 50 years. The most popular and accepted explanation for the formation of ring-banded spherulites is periodic twisting of ribbon-like crystalline lamellae along the radial growth direction of the spherulites.[1−4] Lotz and Cheng extensively studied the origin of lamellar twisting in a comprehensive review, and they believed that unbalanced surface stresses from structural features was the origin for the twisting of lamellae.[5] The rhythmic crystal growth of ring-banded spherulites has been observed experimentally in some polymers,[6−11] but such rhythmic crystal growth is generally encountered in thin films of semicrystalline polymers when the diffusion of molecular chains and the growth of spherulites are competitive because of the mass and spatial confinement.[12] Gazzano et al.[13] and Tanaka et al.[14] confirmed the regular lamellae twisting in poly(3-hydroxybutyrate) (PHB) ring-banded spherulites by microfocus X-ray diffraction. Xu et al.[15] found the lamellae twisting during crystals growth of poly(3-hydroxybutyrate-*co*- 3-hydroxyhexanoate) (PHBHHx) ring-banded spherulites by real-time atomic force microscopy (AFM) observation in thin films. Ho et al.[16] and Wang et al.[17] confirmed the periodical continual twisting of lamellar crystals in poly(trimethylene teraphthalate) (PTT) ring-banded spherulites by electron diffraction (ED).

Although ring-banded spherulites have been widely investigated over the years, analyzing the origin of lamellar twist in ring-banded spherulites remains a challenge because the mere observation of the building lamellae in such complex three-dimensional entities is a difficult task.[5,18] Major contributions to the observation of the internal morphology of spherulites had to await the permanganic acid and potassium hydroxide etching techniques developed by Olley et al.[19,20] In our previous study, a milder methylamine vapor etching technique was developed to provide more clear observation for the lamellar orientation and organization within ring-banded spherulites.[21]

The band spacing of ring-banded spherulites, corresponding to the half-pitch length of twisted lamellae, is the manifestion of lamellar twisting frequency, and it is related to the cause of lamellar twisting. It is generally believed that the band spacing of the semicrystalline polymer ring-banded spherulites increases with crystallization temperature because of the decrease of

Received: November 8, 2010
Revised: February 26, 2011
Published: March 25, 2011

amorphous layer, namely the decrease of unbalanced surface stress, induced by the increase of lamellae regularity.[1] In addition, higher crystallization temperature leads to increase of lamellar thickness, which makes cooperative lamellar twisting more difficult and results in corresponding increase of band spacing. Blending with another polymer also influences the band spacing of ring-banded spherulites. Keith et al.[22] demonstrated that the band spacing of PCL ring-banded spherulites decreased with the increase of PVB fraction in PCL/PVB blends. It is noted that the frequency of lamellar twisting is considerably enhanced because of increased unbalanced surface stress at crystalline lamellar fold surfaces, because the noncrystallizable PVB, which is absorbed on crystal boundaries, actually acts as diluents. Recently, Ho et al.[23,24] found that PS block in PS−PLLA block copolymer decreased the band spacing of PLLA ring-banded spherulites and they believed that crystalline PS−PLLA possessed higher helical twisting frequency for the formation of twisted lamellae due to the effect of PS diluents on PLLA crystalline lamellae. On the other hand, PS segments will also segregate from PLLA segments and the influence of phase separation is very important to the crystallization of long PLLA segments. The decrease of band spacing mentioned above could be attributed to the increased amorphous layer caused by effect of diluents with blending or copolymerization, which make the cooperative lamellar twisting easier. Comparing with blending and block copolymerization, random copolymerization could bring greater effects of amorphous layer and lamellar thickness. In random copolymer, the minor comonomer not only acts as diluents but also change the number-average sequence length of the host polymer, which will significantly decrease the lamellar thickness of the host polymer.[25−27] Introduction of comonomer could also increase the thickness of the disordered layer adjacent to the lamellar folding surface, which will result in the increase of unbalanced stress at the folding surface. So it is expected that incorporation of comonomer will bring great changes of lamellar twisting frequency in polymer ring-banded spherulites.

In this paper, the influence of comonomer segments on the lamellar twisting frequency of PTT ring-banded spherulites was investigated. First, the lamellar morphologies of the PTT ring-banded spherulites were studied by using etching technology. Then, a comonomer, lactide, was introduced into the PTT molecules and the influence of it on the lamellar twisting frequency was discussed.

EXPERIMENTAL SECTION

Materials. Purified terephthalatic acid (PTA) was obtained from Yangzi Petrochemical Company Ltd.. 1,3-propanediol (PDO) was purchased from Cell Ltd. L-lactic acid aqueous solution was obtained from PURAC Ltd. All the other reagents were purchased from Sinopharm Chemical Reagent Co., Ltd.

Synthesis of PTT and PTT-*co*-PLA Copolyesters. PTT was synthesized through two-step process: direct ester interchange of PTA and PDO monomers at 250 °C under 0.3−0.4 MPa with zinc acetate as the catalyst and melt polycondensation at 260 °C under 15 Pa with titanium butoxide as the catalyst. PTT with different molecular weights were obtained.

PTT with $[\eta]$ of 0.51 dL g^{-1}, PLLA with M_w of 5.6 kg mol^{-1} and composite catalysts composed of titanium dioxide, antimonic oxide, polyphospholic acid and tetrabutyl titanate, were placed in a 1 L rotating steel reactor. The reaction blends were kept at 235−240 °C under 10 Pa for 3−5 h. Then, high-molecular-weight PTT-*co*-PLA copolyesters were obtained.

Preparation of Specimen. First, PTT-*co*-PLA copolyester was dissolved in the mixture of chloroform/trifluoroacetic acid (3/1 v/v) and then filtered to eliminate impurity. Then the obtained filtered liquor was precipitated by petroleum ether and filtered in order to remove PLA oligomers and PLA. This process was repeated for three times and then the last filtered cake was collected and dried at 60 °C under vacuum for 48 h.

Specimen for morphologies observation were prepared by casting 15 μL of chloroform/trifluoroacetic acid (3/1 v/v) solution (10 mg mL^{-1}) onto a clean glass slide, which had been preheated to 70 °C, and then films were dried at 60 °C under vacuum for 24 h. Each film on glass slide was isothermally crystallized at special temperature.

Specimen for WAXD and SAXS were made through three steps. First, the sample was made into a film of 215 ± 15 μm by melting the sample between two pieces of polyimide films under 4 MPa. Then the film was placed on a HCS601 microscope hot/cold stage equipped with an Instec STC200 temperature controller and melt at 40 °C above the melting point for 4 min to eliminate the thermal history. Third, the melt sample was quenched to the crystallization temperature at a rate of −250 °C min^{-1} and isothermally crystallized under nitrogen atmosphere for 12 h.

Measurements. The chemical structures of PTT-*co*-PLA copolyesters were characterized using a Bruker AV III 400 MHz nuclear magnetic resonance (NMR) spectrometer. Trifluoroacetic acid-*d* was used as the solvent and all experiments were carried out at 25 °C. Intrinsic viscosities of PTT-*co*-PLA copolyesters in mixture solvents (c = 5 g Dl^{1-}) of phenol and 1,1,2,2-tetrachloroethane (3/2 w/w) were examined using a AV370 Ubbelohde viscometer at 25 °C. Molecular weight and molecular weight distribution of the PTT and copolyesters were measured by Waters-1515 gel permeation chromatography (GPC) with hexafluoroisopropyl alcohol (HFIP) as the solvent at a flow rate of 0.8 mL min^{-1}. The calibration curves were obtained using PS standards.

METTLER TOLEDO−DSC I differential scanning calorimetry (DSC) was employed to detect the heat flow from the samples during isothermal crystallization, nonisothermal crystallization and melting processes. All the experiments were conducted at a rate of 10 °C min^{-1} under nitrogen atmosphere. Melting temperatures (T_m) were taken at the minima of melting endotherms and glass transition temperatures (T_g) at the inflection point.

A Dimension3100 V scanning probe microscope (SPM) and an M-2000DI Ellipsometer were used to measure the thickness of films. The thicknesses were measured to be 1.4 ± 0.3 μm by SPM and 1.49 μm by Ellipsometer with a mean square error (MSE) of 1.57. These measured values are close to the calculated value of 1.53 μm from dividing mass by density and area.

Each film on glass slide was observed using an Olympus BX51 polarized optical microscope (POM) equipped with a CCD camera and a Hitachi TM1000 scanning electron microscopy (SEM) at an accelerating voltage of 15 kV. Before observation of lamellar twisting, the crystal films were treated by a solvent vapor etching using 40% (w/w) methylamine aqueous solution in sealed container at 25 °C.

WAXD at room temperature were acquired by using a Bruker D8 diffractometer, using Ni-filtered Cu Ka radiation at 40 kV and 30 mA. WAXD patterns were recorded in the 2θ range of 5−50° at a scanning rate of 2° min^{-1}. The degree of crystallinity was calculated from the relative areas of the resolved peaks. The lamellar thickness of polymer crystal was investigated by SAXS analysis with a Rigaku RU-200 (Rigaku Corp., Tokyo, Japan), working at 40 kV and 200 mA, with Ni-filtered Cu KR radiation (λ = 0.154 18 nm). The samples were prepared by isothermally crystallized at the setting temperatures for 15 min. SAXS profiles were recorded in the 2θ range 0.1° ∼ 2.5°. Each step increased 2θ by 0.04°, and X-rays were collected for 4 s at each step.

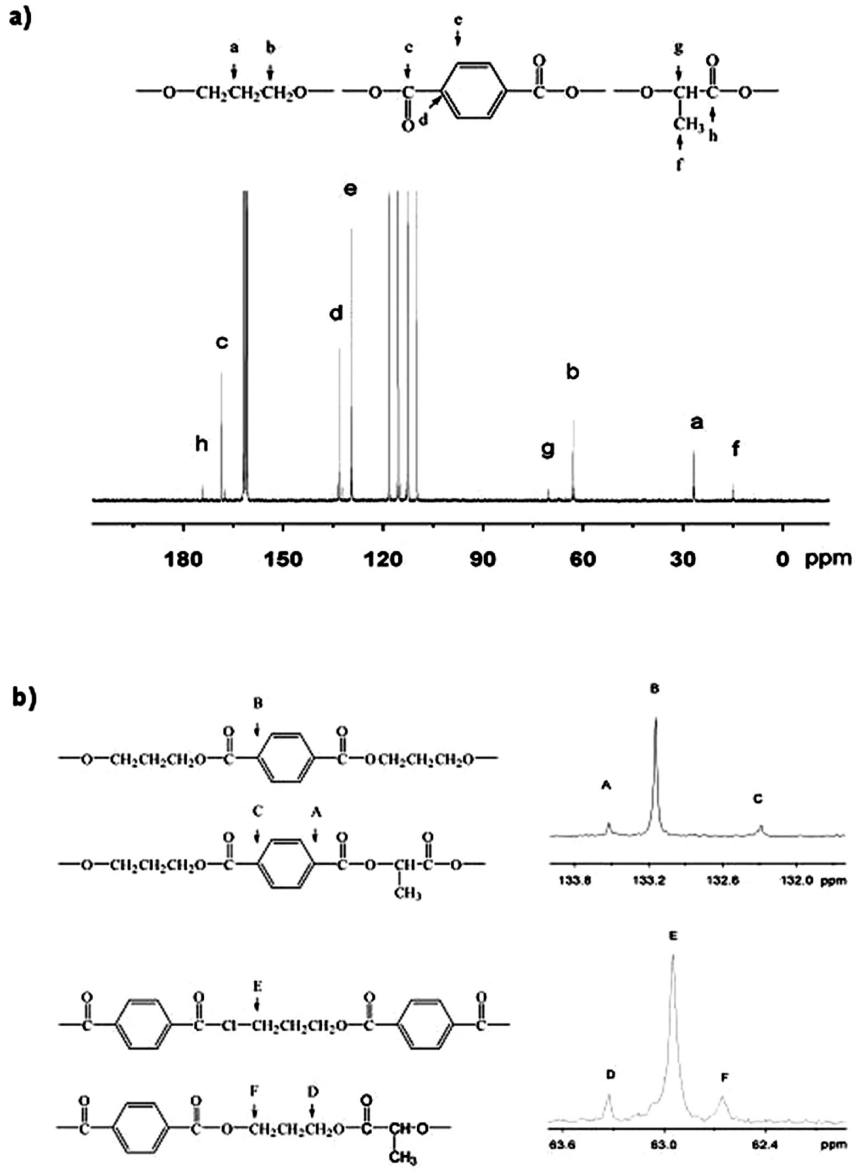

Figure 1. (a) ^{13}C NMR spectrum of PTT-*co*-PLA2 copolyester and the peak assignments. (b) enlarged spectrum in the range of quaternary aromatic carbons d and the methylene carbons a in the $-OCH_2CH_2CH_2O-$ units.

RESULTS AND DISCUSSION

Composition and Properties. Chemical structures of PTT-*co*-PLA copolyesters were characterized with NMR spectrometer. As expected, the reactive blends of PTT oligomer and PLA oligomer were found to generate new TXL, XLT, and XTL sequences, in addition to TX and LL sequences (where X, T, and L represent trimethylene unit from 1,3-propanediol unit, terephthalate unit and lactyl unit, respectively) that present in the initial PTT and PLA homopolymers. As an example, Figure 1a showed the ^{13}C NMR spectrum of PTT-*co*-PLA2 copolyester. The chemical shifts at 62.6−63.3, 26.3−26.8, 68.2−70.9, and 14.7−15.1 ppm were assigned to methylene carbons α (labeled as b) and β (labeled as a) to the ester oxygen in the $-OCHH_2CH_2CH_2O-$ units, the methyl carbons (labeled as f) and methynel carbons (labeled as g) in the lactyl units, respectively. The chemical shifts at 133.4−134.1, 129.4−130.1, 168.7−167.4, and 173.8−174.1 ppm were assigned to those quaternary aromatic carbons (labeled as e), aryl carbons (labeled as d), carbonyl carbons next to the aromatic nucleus (labeled as c) and the carbonyl carbons in the lactyl units (labeled as h), respectively.[28,29] The enlarged ^{13}C NMR spectra in the range of 131.6−134.0 ppm and 61.9−63.7 ppm and the assignments of six peaks are shown in Figure 1b.

The actual terephthalate (T)/lactyl (L) molar ratio of PTT-*co*-PLA copolyester was determined from the relative intensity of aromatic carbon and lactyl methyl carbon resonances. The average number sequence lengths of L units were calculated from the relative intensity of methenyl and methyl carbon resonances of lactyl units,[30] the calculated results are shown in Table 1. It is noted that the PTT sequence length apparently decreased with incorporation of PLA segments.

Molecular weight and molecular weight distribution of the PTT and copolyesters were summarized in Table 1; it can be seen that the molecular weight and molecular weight distribution of PTT-*co*-PLA copolymers is similar. Thermal properties of

Table 1. Composition, molecular weight and thermal properties of PTT and PTT-*co*-PLA

sample	M_L[a] (mol %)	L_L[b]	L_{TT}[c]	$[\eta]$ (dL g^{-1})	M_n (kg mol^{-1})	PDI	T_g (°C)	T_m (°C)
TT1	0	0	14.1	0.14	2.3	1.39	46	225
PTT2	0	0	141.9	0.65	18.6	1.52	47	225
PTT3	0	0	235.8	0.91	41.1	1.76	48	227
PTT-*co*-PLA1	5.8	1.1	9.2	0.97	43.3	1.94	4	217
PTT-*co*-PLA2	12.4	1.2	5.1	0.95	41.6	1.99	47	206
PTT-*co*-PLA3	20.7	1.4	3.8	0.92	40.5	1.96	45	193
PTT-*co*-PLA4	28.4	1.8	3.4	0.88	38.6	2.00	45	179

[a] Mole ratio of lactyl unit. [b] Number-average sequence length of PLA segments. [c] Number-average sequence length of PTT segments.

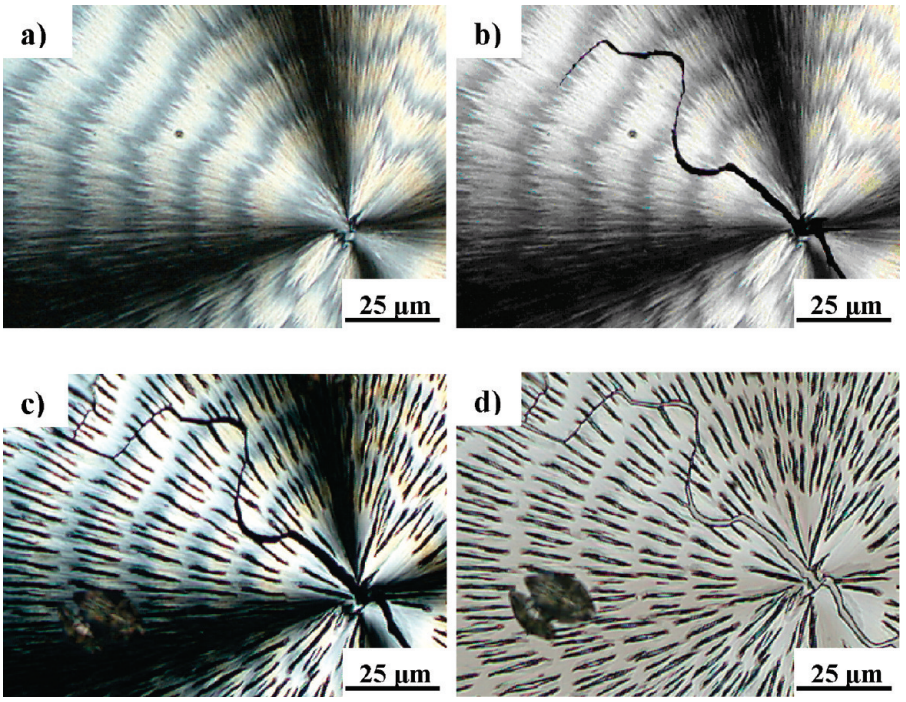

Figure 2. Polarized optical micrographs of PTT1 ring-banded spherulites, formed at 185 °C, etched by methylamine vapor for different times: (a) 0 h, (b) 1 h, (c) 60 h; (d) the optical micrograph of part c.

PTT homopolymers and PTT-*co*-PLA copolyesters were investigated and the results were summarized in Table 1. It can be seen that the melting point (T_m) of PTT decreases with the incorporation of PLA segments, which could be attributed to the decreasing PTT sequence length and chain regularity.

Lamellar Morphologies in Ring-Banded Spherulites. For PTT and PTT-*co*-PLA spherulites obtained at special crystallization temperature, the crystalline lamellae aggregates exhibited ring-banded pattern. Both Maltese cross and extinction rings are clearly observed under crossed-polarized light (Figure 1a), which is similar to the classical ring-banded spherulites in other different polymeric materials. The appearance of ring-banded spherulite is strongly dependent upon crystallization temperature, and the band spacing decreases with the decrease of crystallization temperature, which is same as the results reported by Ho et al.[16] and Wang et al.[17] However, for PTT and PTT-*co*-PLA ring-banded spherulites that crystallized at the same degree of supercooling ($\Delta T = T_m - T_c$), the band spacing of PTT-*co*-PLA ring-banded spherulites is much smaller than that of PTT.

To identify the orientation of lamellar crystals in the ring-banded spherulites, the samples were etched by methylamine vapor and studied in detail. Figure 2 shows the POM images of PTT ring-banded spherulites etched for 0, 1, and 60 h, respectively. It can be seen that the etching starts from the central of the spherulites. The reason for this phenomenon is that the spherulitic eyes at the central part of spherulites are thinner and more easily eroded by methylamine than lamellar crystals in other regions. Similar phenomena were found in our previous study on the etching of PHBV ring-banded spherulites.[21] After long time etching, many slits along the radius direction appear because the regions between edge-on lamellae are easier to be etched and washed out (Supporting Information, Figure S1). It should be noted that similar results were obtained in the etched PTT-*co*-PLA ring-banded spherulites.

The twisting of lamellae can be distinctly seen in SEM images of etched PTT and PTT-*co*-PLA ring-banded spherulites, as shown in Figure 3. As suggested by Keith and Padden,[1] nonadjacent re-entry of chains and loose folds generally introduce overcrowding and inefficient packing in lamellar crystals. The different conditions at the opposite fold surfaces may lead to the difference in the magnitude of compressive stresses, which can result in a bending moment responsible for twisting of lamellar

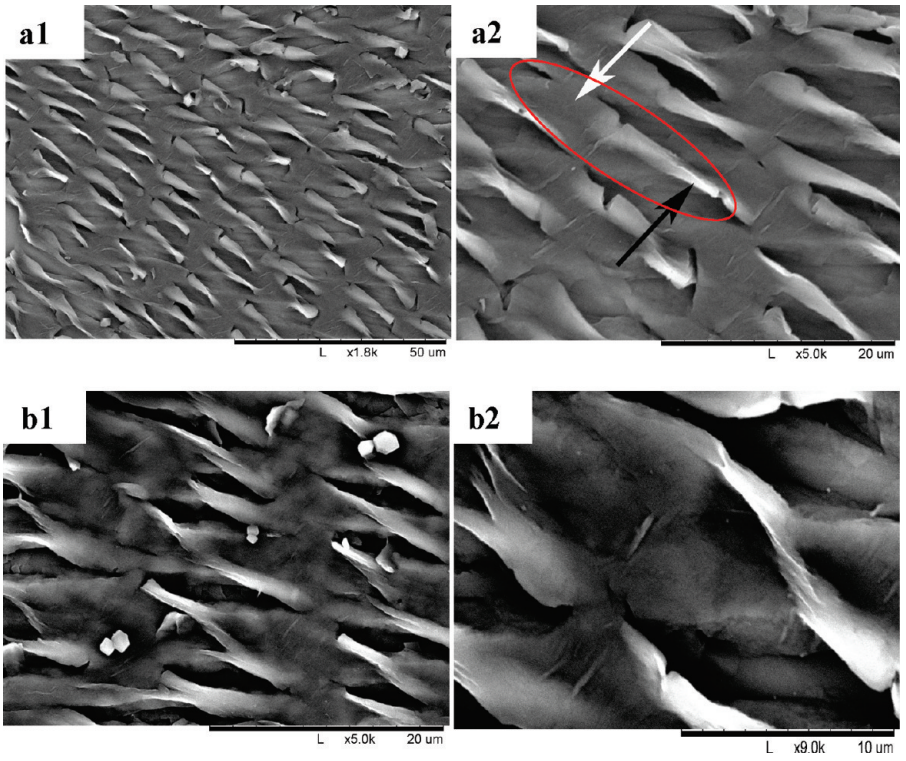

Figure 3. SEM images of PTT3 ring-banded spherulites (crystallized at ΔT of 40 °C) etched by methylamine vapor for 360 h (a1 and a2) and PTT-*co*-PLA1 ring-banded spherulites (crystallized at ΔT of 30 °C) etched by methylamine vapor for 300 h (b1 and b2).

crystals. It can be seen in Figure 3a2, edge-on lamellar crystals (the black arrow) protrude from the film surface, after growing to a certain length edge-on lamellae twist and lamellae with tilt orientation can be seen, and the lamellae twist to the flat-on lamellar crystals (the bright arrow) with further growth. The continual periodical lamellar twisting in PTT ring-banded sphrulites can be confirmed by SEM images in Figure 3a, which is consistent with the results obtained by Ho et al.[16] and Wang et al.[17] using transmission electron microscopy (TEM) and ED. In etched PTT-*co*-PLA ring-banded spherulites, obvious periodical cooperative twisting of lamellar crystals can also be seen, as shown in Figure 3b. The alternating flat-on-to-edge-on morphologies are consistent with the alternating dark-to-bright bands in POM images. It was found that same twist orientations of lamellar crystals were observed in PTT and PTT-*co*-PLA ring-banded spherulites.

The Influence of Comonomer and Sequence Length on Ring-Banded Spherulites. To investigate whether PLA segments in the PTT-*co*-PLA copolyesters crystallize at the setting crystallization temperatures, PTT and PTT-*co*-PLA samples crystallized at different temperatures were studied by WAXD. All PTT-*co*-PLA copolyesters show the same crystalline diffraction peaks as PTT homopolymer[17] and the diffraction peaks do not change with crystallization temperature, and no crystalline diffraction peaks corresponding to PLA crystal was found (Supporting Information, Figure S2). Therefore, it can be concluded that PTT-*co*-PLA has the same crystalline structures as PTT and PLA segments are in amorphous state.[28]

To study the influence of amorphous PLA segments on the ring-banded spherulites, the band spacing of PTT and PTT-*co*-PLA ring-banded spherulites was investigated. The influence of sequence length (namely molecular weight in homopolymers) on band spacing has been studied in many homopolymers, and band spacing generally decreases with the increase of sequence length.[3,31] However, to our knowledge, the influence of comonomer on ring-banded spherulites of random copolymer that show no cocrystallization behavior has not been studied yet. Three PTT and four PTT-*co*-PLA samples, with different number-average sequence length, were studied. The typical morphologies of PTT and PTT-*co*-PLA ring-banded spherulites crystallized at different ΔT are shown in Figure 4. The appearance of ring-banded spherulites in PTT and PTT-*co*-PLA is strongly dependent upon ΔT and the band spacing decreases with the increase of ΔT. It is also noted that the band spacing and regularity of ring bands decreases with the increase of lactyl units content. The measured band spacing results of all samples were summarized in Figure 5. As can be seen in Figure 5, PTT-*co*-PLA ring-banded spherulites show apparently smaller band spacing than PTT ring-banded spherulites. For example, the band spacing of PTT1 ring-banded spherulites crystallized at ΔT of 40 °C was 25.15 μm while that of PTT-*co*-PLA4 ring-banded spherulites crystallized at the same ΔT was only 1.78 μm. Moreover, the band spacing of PTT ring-banded spherulites slightly decreases with the increase of molecular weight (sequence length), while the band spacing of PTT-*co*-PLA ring-banded spherulites sharply decreases with the increase of the lactyl units content and the correlative sequence length. From the results mentioned above, PTT-*co*-PLA copolyesters possess greater helical twisting frequency than PTT homopolymer, and the higher the content of PLA segments content, the greater the frequency. Similar phenomenon has been reported in block copolymer of PS−PLLA in which introduction of PS block increases the helical twisting frequency and decreases the band spacing of PLLA ring-banded spherulites.[24]

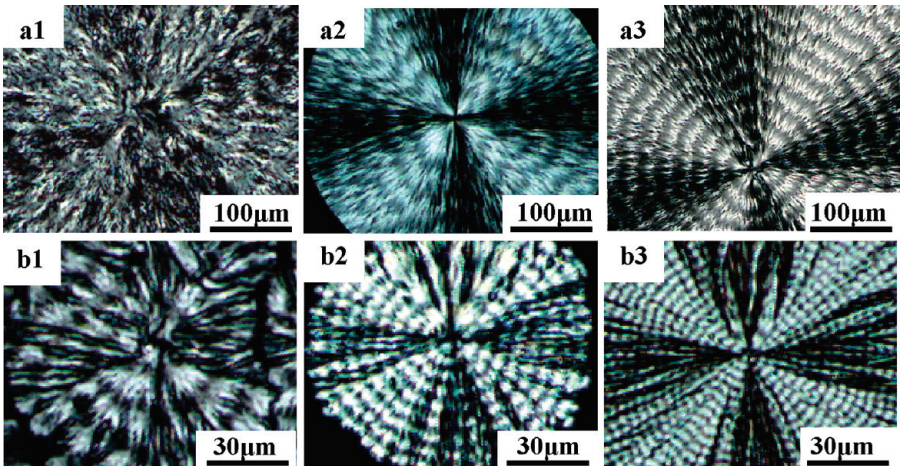

Figure 4. POM images of PTT1 (a) and PTT-*co*-PLA3 (b) ring-banded spherulite obtained at different degree of supercooling: (a1, b1) ΔT = 20 °C; (a2, b2) ΔT = 30 °C; (a3, b3) ΔT = 40 °C.

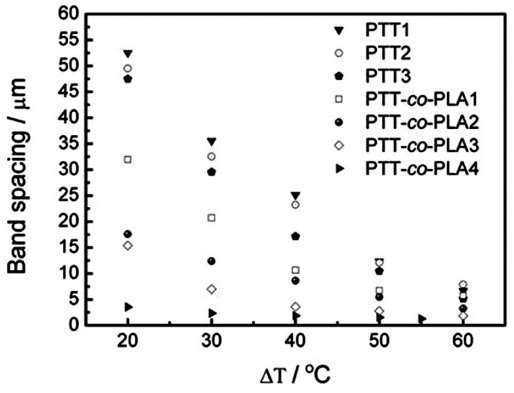

Figure 5. Crystallization temperature dependency of band spacing for ring-banded spherulites of PTT with different sequence length and PTT-*co*-PLA copolyesters with different PLA segments content.

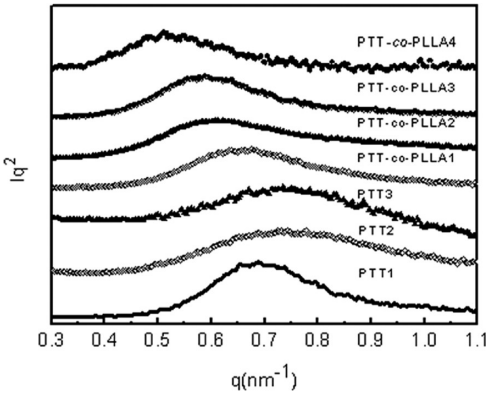

Figure 6. SAXS patterns of PTT and PTT-*co*-PLA thin films crystallized at ΔT of 40 °C.

To further study the influence of amorphous PLA segments on PTT ring-banded spherulites, the thickness of lamellar crystals and the thickness of amorphous layer in PTT and PTT−PLA ring-banded spherulites were measured by SAXS. PTT and PTT-*co*-PLA thin films, with thickness of 215 ± 15 μm, crystallized at ΔT of 40 °C, were used for SAXS. Each sample showed similar ring-banded morphologies but a litter lower degree of crystallinity compared to its solution casting films on the glass slide, but the influence of the slight difference in degree of crystallinity on the calculation of lamellar thickness is in acceptable range. SAXS patterns are shown in Figure 6, and only one maximum was observed in each Lorentz-corrected SAXS profile. As demonstrated by Crist,[32] it is well justified to use the first scattering maximum to calculate the average structural period of the lattice (long period) in such conditions. Assuming a simple two-phase model of the semicrystalline PTT and PTT-*co*-PLA, the thickness of lamellar crystals (L_c) and the thickness of amorphous layer (L_a) can be estimated by the product of L and the volume fraction of crystal, X_v, which is calculated from the mass fraction of the crystal, X_m. And it is safe to assume that $X_m \approx X_w$ since the electron density is approximately proportional to the mass. Hence, X_v is determined by eq 1.[33]

$$X_V = \frac{\rho_a}{X_w\rho_a + (1 - X_w)\rho_c} X_w \qquad (1)$$

Here X_w is obtained by WAXD, and ρ_a and ρ_c are the amorphous and crystalline densities, respectively. The amorphous and crystalline densities of PTT at 25 °C were reported to be 1.2990 and 1.4412 g cm^{-3}, respectively,[16,34] and those of PLA were reported to be 1.2480 and 1.2900 g cm^{-3}, respectively.[35] The crystal density ρ_c for PTT-*co*-PLA with PTT type crystal was estimated as the density of PTT crystal. The amorphous density ρ_a for PTT-*co*-PLA was estimated as the density of the blend of amorphous PTT and PLA by plotting ρ_a against M_{PLA},[36] and the results are ρ_a = 1.2990 − 0.058 M_{PLA}. Therefore, we estimated the thickness of lamellar crystals (L_c) as a product of L and X_v and the thickness of amorphous layer (L_a) as ($L - L_c$).[33,37] L, L_c, and L_a for PTT and PTT-*co*-PLA ring-banded spherulites were summarized in Table 2. It can be seen that the lamellar crystals thickness of PTT homopolymer is about 3.6 nm, which is similar to the results reported by Hong et al..[38] The L_c of PTT-*co*-PLA copolymers were calculated to be 2.2−3.6 nm, which was similar to the results by using the first-dimension correlation function method (L_c = 3.5−3.9 nm). It can also be seen that L_c decreases with the increase of PLA segments, which is corresponding to the results that the melting temperature (T_m) of PTT-*co*-PLA decreases with the increase of PLA segments content (Table 1).[39,40] It is should be noted that PLA segments had greater influence on the PTT lamellar thickness than molecular weight. The increase of L and L_a with PLA segments should be attributed to the decreasing PTT

Table 2. Degree of Crystallinity and the Thickness of Different Phases in PTT and PTT-*co*-PLA Ring-Banded Spherulites

number	X_v (%)	q_{max1} (nm^{-1})	L (nm)	L_c (nm)	L_a (nm)
PTT1	45	0.68	9.2	4.1	5.1
PTT2	43	0.75	8.4	3.6	4.8
PTT3	41	0.73	8.6	3.5	5.1
PTT-*co*-PLA1	30	0.66	9.5	2.9	6.6
PTT-*co*-PLA2	27	0.61	10.3	2.7	7.6
PTT-*co*-PLA3	23	0.59	10.6	2.5	8.2
PTT-*co*-PLA4	18	0.53	11.8	2.2	9.7

sequence length and chain regularity and correlative degree of crystallinity, which is similar to the influence of poly(ethylene oxide) segments on the poly(trimethylene terephthalate) that was reported by Szymczyk.[25]

Origins for the Change of Lamellar Twisting Frequency in PTT-*co*-PLA Ring-Banded Sperulites. It is generally believed that the occurrence of ring-banded spherulites is attributed to the periodical cooperative lamellar twisting along the radial direction. Considering a polymer lamellae as a cantilever with thickness of b,[3] the disparate compressive stresses on the folding surface, τ, cause a torque of T and a bending with a angular rotation θ per unit. It can be found that the angular rotation between two cross sections per unit distance, θ, can be calculated by eq 2.[41]

$$\theta = \frac{T}{Ghb^3\left[\frac{1}{3} - 0.21\frac{b}{h}\left(1 - \frac{b^4}{12h^4}\right)\right]} = \frac{T}{C_1 Ghb^3} \qquad (2)$$

where G is the elastic modulus, h is the width, b is the thickness, and C_1 can be calculated by using the h/b value (when h/b is more than 10, C_1 is less than 0.333). Equation 2 indicates that θ, which is directly proportional to the twisting frequency, increases with T and decreases with h and b. The θ, in a thin plate with compressed surface layer, is generally proportional to its thickness, which has been observed in thin films of metals.[42] For the thin PTT lamellae, the twisting sense can also be analyzed using eq 2.

In PTT-*co*-PLA ring-banded spherulites mentioned above, only PTT chains crystallize to form crystalline lamellae, the region between the lamellae is occupied by amorphous PTT and PLA segments. According to the mechanism proposed by Keith and Padden, steric hindrance or chain tilt could result in the unbalanced surface stress and the corresponding curvature of polymer crystals.[1,43,44] PTT crystal is two-chain triclinic structure,[16] so an unbalanced surface stress, which leads to the crystalline lamellar curvature, is initiated by imbalance of fold geometry or conformation and improved by polymer chains overcrowding and inefficient packing at crystalline lamellar fold surfaces. Therefore, an unbalanced surface stress at the fold surfaces should also be expected in PTT-*co*-PLA copolyesters.

As illustrated, the unbalanced surface stress is initiated by imbalance of fold geometry or conformation. Moreover, the unbalanced surface stress is intensified by the effect of diluents due to the existence of dangling amorphous PLA segments. In particular, the PLA random chains, dangling from PTT crystalline lamellar surface via chemical junction, can be regarded as the origin for the amplification of steric hindrance effect due to the formation of phase separation resulting from incompatibility. So we speculate that the stress loaded on the PTT lamellae, τ, is promoted by the incorporation of PLA segments, which is the main reason for the increasing lamellar twisting frequency with PLA segments in PTT-*co*-PLA ring-banded spherulites.

At the same time, incorporation of PLA segments increases the amorphous layer thickness, which will result in the increase of unbalanced surface stress, and decreases the lamellar thickness. As mentioned above (Table 2), the thickness of amorphous layer and crystalline lamellae in PTT-*co*-PLA4 were increased to 190% and decreased to 60% of that in PTT, respectively. Roughly estimated with eq 2, even if the stress was constant, the angular rotation per unit in the PTT-*co*-PLA4 lamellae will be increased to about 600% of that in PTT.

Consequently, the sharp decrease of the band spacing in PTT-*co*-PLA ring-banded spherulites can be regarded as the cooperative effect of increasing unbalanced surface stress and the decrease of lamellae thickness. The effect of steric hindrance that causes unbalanced surface stress was intensified by the incorporation of PLA segments and the decrease of lamellae thickness, which lead to significant lamellar twisting so as to result in the ring-banded spherulites with higher twisting frequency.

CONCLUSION

A series of random PTT-*co*-PLA copolyesters were synthesized to study the influence of PLA segments on the lamellar twisting frequency in PTT ring-banded spherulites. It was found that PLA segments did not crystallize in PTT-*co*-PLA crystalline films. The periodical cooperative twisting of lamellar crystals in PTT and PTT-*co*-PLA ring-banded spherulites was clearly observed by using mild methylamine steam etching method. Compared with ring-banded spherulites in PTT homopolymer, PTT-*co*-PLA ring-banded spherulites had much smaller band spacing, and the band spacing decreased with the increase of PLA segments content. The reason for the sharp decrease in band spacing was analyzed on the basis of the theory of unbalanced stress leading to lamellae twisting, proposed by Keith and Padden. One is the intensified unbalanced surface stress at the fold surfaces by PLA segments due to the effect of diluents on the formation PTT lamellae. Another one is the decrease of crystalline lamellae thickness. Both changes significantly enhance the helical twisting frequency of lamellae. The model to explain the formation of PTT-*co*-PLA ring-banded spherulites may provide further understanding for the formation of other polymer ring-banded spherulites.

ASSOCIATED CONTENT

Supporting Information. Surface morphology of PTT ring-banded spherulites by SEM, AFM, and WAXD. This material is available free of charge via the Internet at http://pubs.acs.org.

AUTHOR INFORMATION

Corresponding Author

*E-mail: (Q.G.) guqun@nimte.ac.cn; (Z.W.) wangzb@nimte.ac.cn.

ACKNOWLEDGMENT

This work was supported by the National Science Foundation of China (21004073), National Key Technology R&D Program

(2007BAE28B06), and China Postdoctoral Science Foundation (20090450084), Natural Science Foundation of Ningbo Municipal (2006A610071), Ningbo Natural Science Foundation (2010A610193), and Program for Ningbo Innovative Research Team (Grant No. 2009B21008) is greatly appreciated. We also would like to thank Professor Yong-feng Men of the Chang Chun Institute of Applied Chemistry, Chinese Academy of Sciences for his help with SAXS analysis.

REFERENCES

(1) Keith, H. D.; Padden, F. J., Jr *Polymer* **1984**, *25* (1), 28–42.
(2) Keith, H. D.; Padden, F. J.; Lotz, B.; Wittmann, J. C. *Macromolecules* **1989**, *22* (5), 2230–2238.
(3) Keith, H. D.; Padden, F. J. *Macromolecules* **1996**, *29* (24), 7776–7786.
(4) Keith, H. D.; Chen, W. Y. *Polymer* **2002**, *43* (23), 6263–6272.
(5) Lotz, B.; Cheng, S. Z. D. *Polymer* **2005**, *46* (3), 577–610.
(6) Duan, Y.; Jiang, Y.; Jiang, S.; Li, L.; Yan, S.; Schultz, J. M. *Macromolecules* **2004**, *37* (24), 9283–9286.
(7) Duan, Y.; Zhang, Y.; Yan, S.; Schultz, J. M. *Polymer* **2005**, *46* (21), 9015–9021.
(8) Wang, Z.; Hu, Z.; Chen, Y.; Gong, Y.; Huang, H.; He, T. *Macromolecules* **2007**, *40* (12), 4381–4385.
(9) Wang, Z.; Alfonso, G. C.; Hu, Z.; Zhang, J.; He, T. *Macromolecules* **2008**, *41* (20), 7584–7595.
(10) Chen, J.; Yang, D. *Macromolecules* **2005**, *38* (8), 3371–3379.
(11) Wang, Y.; Chan, C.-M.; Li, L.; Ng, K.-M. *Langmuir* **2006**, *22* (17), 7384–7390.
(12) Keith, H. D. *Polymer* **2001**, *42*, 9987–9993.
(13) Gazzano, M.; Focarete, M. L.; Riekel, C.; Scandola, M. *Biomacromolecules* **2000**, *1* (4), 604–608.
(14) Tanaka, T.; Fujita, M.; Takeuchi, A.; Suzuki, Y.; Uesugi, K.; Doi, Y.; Iwata, T. *Polymer* **2005**, *46* (15), 5673–5679.
(15) Xu, J.; Guo, B.-H.; Zhang, Z.-M.; Zhou, J.-J.; Jiang, Y.; Yan, S.; Li, L.; Wu, Q.; Chen, G.-Q.; Schultz, J. M. *Macromolecules* **2004**, *37* (11), 4118–4123.
(16) Ho, R.-M.; Ke, K.-Z.; Chen, M. *Macromolecules* **2000**, *33* (20), 7529–7537.
(17) Wang, B.; Li, C. Y.; Hanzlicek, J.; Cheng, S. Z. D.; Geil, P. H.; Grebowicz, J.; Ho, R.-M. *Polymer* **2001**, *42* (16), 7171–7180.
(18) Organ, S. J. B.; P, J. *J. Mater. Sci. Lett.* **1989**, *8*, 621–623.
(19) Olley, R. H.; Hodge, A. M.; Bassett, D. C. *J. Polym. Sci., Polym. Phys. Ed.* **1979**, *17* (4), 627–643.
(20) Bassett, D. C.; Olley, R. H. *Polymer* **1984**, *25* (7), 935–943.
(21) Wang, Z.; Li, Y.; Yang, J.; Gou, Q.; Wu, Y.; Wu, X.; Liu, P.; Gu, Q. *Macromolecules* **2010**, *43* (10), 4441–4444.
(22) Keith, H. D.; Padden, F. J.; Russell, T. P. *Macromolecules* **1989**, *22* (2), 666–675.
(23) Ho, R. M.; Chen, C. K.; Chiang, Y. W.; Ko, B. T.; Lin, C. C. *Adv. Mater.* **2006**, *18* (18), 2355–2358.
(24) Chao, C.-C.; Chen, C.-K.; Chiang, Y.-W.; Ho, R.-M. *Macromolecules* **2008**, *41* (11), 3949–3956.
(25) Szymczyk, A. *Eur. Polym. J.* **2009**, *45* (9), 2653–2664.
(26) Kint, D. P. R.; Alla, A.; Deloret, E.; Campos, J. L.; Munoz-Guerra, S. *Polymer* **2003**, *44* (5), 1321–1330.
(27) Baratian, S.; Hall, E. S.; Lin, J. S.; Xu, R.; Runt, J. *Macromolecules* **2001**, *34* (14), 4857–4864.
(28) He, A.; Han, C. C.; Yang, G. *Polymer* **2004**, *45* (24), 8231–8237.
(29) Szymczyk, A. *Eur. Polym. J.* **2009**, *45* (9), 2653–2664.
(30) Newmark, R. A. *J. Polym. Sci.: Polym. Chem. Ed.* **1980**, *18* (2), 559–563.
(31) Wang, Y.; Mano, J. F. *J. Appl. Polym. Sci.* **2007**, *105* (6), 3500–3504.
(32) Crist, B. *J. Polym. Sci., Polym. Phys. Ed.* **1973**, *11* (4), 635–661.
(33) Yoshie, N.; Saito, M.; Inoue, Y. *Macromolecules* **2001**, *34* (26), 8953–8960.
(34) Grebowicz, J. S.; Brown, H.; Chuah, H.; Olvera, J. M.; Wasiak, A.; Sajkiewicz, P.; Ziabicki, A. *Polymer* **2001**, *42* (16), 7153–7160.
(35) Mark, J. E. Polymer Data Handbook, Oxford University Press, Inc.: Oxford, U.K., 1999.
(36) Barker, P. A.; Mason, F.; Barham, P. J. *J. Mater. Sci.* **1990**, *25* (4), 1952–1956.
(37) DiMarzio, E. A.; Guttman, C. M.; Hoffman, J. D. *Macromolecules* **1980**, *13* (5), 1194–1198.
(38) Hong, P.-D.; Chuang, W.-T.; Yeh, W.-J.; Lin, T.-L. *Polymer* **2002**, *43* (25), 6879–6886.
(39) Lotti, N.; Finelli, L.; Fiorini, M.; Righetti, M. C.; Munari, A. *Polymer* **2000**, *41* (14), 5297–5304.
(40) Ko, C.-Y.; Chen, M.; Wang, H.-C.; Tseng, I. M. *Polymer* **2005**, *46* (20), 8752–8762.
(41) Gere, J. M.; Goodno, B. J. *Mechanics of Materials, 7th*. Cengage Learning, Inc., **2009**, 228.
(42) Bowden, N.; Brittain, S.; Evans, A. G.; Hutchinson, J. W.; Whitesides, G. M. *Nature* **1998**, *393* (6681), 146–149.
(43) Lovinger, A. J.; Keith, H. D. *Macromolecules* **1996**, *29* (26), 8541–8542.
(44) Keith, H. D.; Padden, F. J. *Macromolecules* **1996**, *29* (24), 7776–7786.